

# Galaxy Formation in Hierarchical Models

F J SUMMERS

Princeton University Observatory, Peyton Hall, Princeton, NJ 08544  
summers@astro.princeton.edu

## ABSTRACT

High resolution gravity plus smoothed particle hydrodynamics simulations are used to study the formation of galaxies within the context of hierarchical structure formation. The simulations have sufficient dynamic range to resolve from ten kpc scale galactic disks up to many Mpc scale filaments. Over this range of scales, we find that hierarchical structure development proceeds through a series of increasingly larger filamentary collapses. The well resolved simulated galaxies contain hundreds to thousands of particles and have varied morphologies covering the entire expected range from disks to tidally distorted objects. The epoch of galaxy formation occurs early, about redshift 2.5 for  $10^{12} M_{\odot}$  galaxies. Hierarchical formation naturally produces correlations among the mass, age, morphology, and local density of galaxies which match the trends in the observed morphology–density relation. We also describe a method of spiral galaxy formation in which galactic disks form through the discrete accretion of gas clouds which transport most of the angular momentum to the inner regions. Such a process is characteristic of the somewhat chaotic nature of hierarchical structure formation where simple analytical ideas of spherical collapse appear incongruous.

*Subject headings:* cosmology: large-scale structure of universe — galaxies: clustering — galaxies: formation

## 1. Introduction

In a previous paper (Evrard, Summers, & Davis 1994, hereafter Paper I), we demonstrated the ability to resolve galaxies within cosmological simulations. In particular, we established that an abundant population of galaxy-like objects are easily defined, that these simulated galaxies have sizes and masses characteristic of real galaxies, and that galactic disks can form naturally from hierarchical initial conditions. This paper extends that work by examining the processes of galaxy formation more closely.

The simple analytic picture of galaxy formation considers an individual collapsing gas cloud (e.g., Eggen, Lynden-Bell, & Sandage 1962). A cloud is Jeans unstable to collapse when its gravitational collapse time scale becomes shorter than the timescale for pressure response. When the timescale for cooling the gas is shorter than the free fall time scale, the cloud can fragment into smaller pieces, presumably leading to eventual star formation (Gott & Thuan 1976; Rees & Ostriker 1977; Silk 1977). The timing of star formation during the collapse is important for the morphology of the galaxy. Spiral galaxies have disks of young stars with low velocity dispersions and star formation there must occur after

the disk has formed. In ellipticals, with old stellar populations and shapes determined by large velocity dispersions, star formation must occur early in the process. It has been suggested for some time that ellipticals may form via mergers and interactions rather than by single cloud collapse (Toomre & Toomre 1972; Barnes & Hernquist 1992).

Disk formation is seen as the natural result of collapse of a cloud with non-zero angular momentum. Centrifugal forces of rotation lead to preferential collapse along the direction parallel to the rotation axis. The cloud must remain gaseous, hence collisional, during this collapse for a thin disk to form. The collapse in the plane of the disk continues until the disk is rotationally supported against the gravitational potential. The caveat to this picture is the creation of the initial angular momentum of the cloud and large scale tidal torques are often invoked to explain this (see e.g., Efstathiou & Silk 1983).

Hierarchical structure formation will alter this basic picture considerably. The simplistic idea of a coherent collapse of a single cloud gives way to a picture in which small scale objects collapse first, and then merge into successively larger objects. The relevant Jeans and cooling criteria address the current level of the hierarchy and not the entire collapsing region. The timescales between each stage of building this hierarchy are sufficiently close to the collapse timescales that one does not know whether a level of structure will reach an equilibrium before it is incorporated into the next higher level. The emphasis on merging might interfere with disk formation or disrupt already formed disks (Paper I; Toth & Ostriker 1992; Navarro, Frenk, & White 1994). Hierarchical construction also may mean that large mass ellipticals are assembled too late to fit with observations.

There have been many analytical and semi-analytical treatments of hierarchical galaxy formation (e.g., White & Frenk 1991; Kauffmann, White, & Guiderdoni 1993; Lacey & Cole 1993). A statistical description of galaxy formation can be created which reproduces many of the observations. Some limitations of these methods are that the important processes must be identified in advance and that it is difficult to incorporate complex feedback processes. Additionally, one does not obtain a detailed look at the processes or gain insight into the dynamical aspect.

Numerical simulations have become a useful tool for examining the interaction of processes in a dynamical setting. Simulations of isolated galaxy collapses (e.g., Katz & Gunn 1991; Steinmetz & Mueller 1994) require simplifying assumptions such as spherical clouds and solid body rotation to create initial conditions. Compared to the present work, other simulations which start with cosmological initial conditions have either not had the resolution to consider morphologies (Katz, Hernquist, & Weinberg 1992), or have studied a limited number of targeted objects (Navarro & White 1994). The above references and Paper I have shown that gas can cool efficiently (perhaps too efficiently) to galactic overdensities and that galactic disks can form naturally in hierarchical models. Such work, including this paper, is limited by an incomplete physical model and limited dynamic range. The goal of resolving galaxies within a region large enough to statistically test cosmological models and including the diverse physical processes required has fostered

several supercomputing research groups.

This paper is organized as follows. §2 presents a brief overview of the simulation, examines some characteristics of hierarchical formation, and demonstrates the dynamic range available in the numerical model. We then explore the various simulated galaxy morphologies and their dependence upon environment. In §4, we consider the timing of galaxy formation and its relation to other galaxy characteristics. The detailed description of the formation of a galaxy with a strong disk and the implications for spiral galaxy formation are covered in §5. Discussion of our results within larger contexts rounds out the paper.

## 2. Simulation Overview

The numerical details of the simulation were presented in Paper I. Only a brief description will be given here. The simulation follows the coupled evolution of dark matter and baryonic particle fluids with the P3MSPH code (Summers 1993; Evrard 1988). Initial conditions are chosen from a CDM power spectrum with cosmological density parameter  $\Omega = 1$ , present Hubble parameter  $h = 0.5$  in units of  $100 \text{ km s}^{-1} \text{ Mpc}^{-1}$ , and normalization of  $\sigma_8 = 0.6$ , where  $\sigma_8$  is the linearly predicted rms fluctuation within  $8 \text{ h}^{-1} \text{ Mpc}$  radius spheres. 262,144 particles per species are tracked within a cubical region with comoving side length,  $L$ , of 16 Mpc. The simulated region is constrained to contain a mass concentration characteristic of a poor cluster of galaxies in the center. The timestep is 6.1 Myr, the resolution scale is  $\sim 20/(1+z)$  kpc, and the particle masses are  $9.72 \times 10^8 M_\odot$  and  $1.08 \times 10^8$  for the dark matter and baryonic particles, respectively. The baryonic species is governed by the equations of smoothed particle hydrodynamics (SPH) which includes radiative cooling for a primordial composition gas. The simulation is designed to cover the smaller scales of cosmology ( $\sim 10 \text{ Mpc}$ ) down to the larger scales of galaxies ( $\sim 10 \text{ kpc}$ ).

Specific limitations of the simulation were also described in Paper I (see §2.2), but a few comments bear mention here as well. First, resolution constraints do not allow us to see structure forming on scales below  $3 \times 10^{10} M_\odot$ . The first resolvable objects are about the size of the Large Magellanic Cloud. In as much as the information from smaller scales is forgotten when the resolvable structures form, our simulation picks up the formation in progress. Second, the assumed cosmology does not match the normalization predicted by the COBE observations (Efstathiou, Bond, & White 1992). Accordingly, this paper does not attempt to produce global tests of the CDM model, but rather focuses on the characteristic processes in any hierarchical structure formation model. The important point is that the power spectrum falls roughly as  $P(k) \propto k^{-2}$  on galaxy scales. The simulation can essentially be scaled to match the normalization of a desired model by considering it to occur at a different epoch. Third, we do not include radiative heating from an ionizing background. This energy input would only affect the smaller objects and the very efficient cooling found in the large objects would not be altered (Katz, Weinberg, & Hernquist 1996). Fourth, and most important, is the omission of star formation. Our

simulation does not identify when star formation occurs during the collapse process and is strictly correct only during the gaseous phase of collapse. Delving into star formation will add a new set of parameters to the simulation model and will be explored in a subsequent paper. It is important to define the situation with well known physics before pushing into areas that are less well constrained on these scales.

Figure 1 presents the time development of structure in the simulation. A slice of dimensions  $L \times L \times 0.2L$  shows the principle collapse plane of the poor cluster of galaxies. The dominant object is the cluster halo in the central region. It contains a dark matter mass of about  $5.5 \times 10^{13} M_{\odot}$  within a virial radius of 486 kpc (defined by an overdensity of 200) at the end of the simulation. A group of galaxies forms above and to the right of center. It has a final virial mass of  $1.6 \times 10^{13} M_{\odot}$  within 319 kpc. No doubt if the simulation were continued, this group would eventually merge with the central cluster. Many galaxy scale structures appear throughout the box. Most are concentrated in filamentary structures, but some appear in relatively low density environments (though one must be careful because these plots are projected slices). The sizes of the filaments and voids are limited only by the size of the simulation.

The development of linear structures, generically called filaments, illustrates the hierarchical nature of the process. At early times there are many short segments connected in a kinked fashion to a few longer sections. As time progresses, the kinked regions collapse into bound structures and the filaments become longer and straighter. Additionally, collapse occurs within the filaments themselves and their appearance changes from continuous to dotted to clumpy. It has been noted before that groups and clusters form at the vertex of several filaments, but note here how the formation of the cluster helps strengthen and define the alignment of the filaments. It is a dual process that creates both the cluster and the aligned filaments in tandem. The generalization of this idea is that, at any given stage of structure development, filaments should connect the dominant collapsed structures. These filaments will reflect the progression of hierarchical collapse in their transition from shorter to longer, kinked to straight, and continuous to clumpy.

When concentrating on the high density structures, one follows the collapse of positive mass perturbations and the process of collecting them together into larger structures. Alternatively, one can reverse the foreground and background by following the expansion of negative mass fluctuations, or voids. The theoretical advantage is that void regions obey the linear theory equations. The practical advantage can be seen by tracking the voids in Figure 1. While the voids at the end of the simulation are apparent back to the initial conditions, the final positions of the overdense structures do not correlate well with their initial positions. This suggests that describing large scale structure by expansion and merging of voids might be analytically fruitful because the centers of voids are relatively stationary. It also illustrates the problems entailed in reconstruction methods for determining the initial perturbation field (Weinberg 1992). Many stages of the hierarchy have become mixed and are cloaked by the final cluster halo.

Although only the dark matter is shown in Figure 1, the baryons trace the same structures on these scales (see Paper I, Fig. 3). Above 1 Mpc, there is no evidence for segregation of the baryons and the dark matter. Indeed, as the collapse is pressureless until a shock is reached, no segregation should be expected. The Mpc scale demarks the point where hydrodynamic effects become of the same order as gravitational effects for this simulation. On smaller scales, hydrodynamics is required for a correct description.

This assertion is punctuated by the dynamic range comparison in Figure 2. The top row exemplifies why dark matter simulations are unsatisfying for galaxy formation studies. The dark matter structures that look interesting in one panel appear bland in the panel to the right. The 400 kpc panel reveals that the cluster halo has almost no sub-structure and the galactic halo in the 70 kpc panel is difficult to identify. In contrast, the baryons show a richness of structure on all three levels. The cluster halo is populated by an assortment of simulated galaxies. The galactic scale dark matter halo surrounds a collapsed baryonic galaxy much as envisioned by, for example, White & Rees (1978). This figure affirms the simulation aim of modelling structure from a several kpc to a several Mpc.

The results of this section show that the simulation is adequate to the task of addressing galaxy formation in a cosmological context. The large scales of the simulation exhibit the characteristics of hierarchical structure formation. The wide dynamic range and high spatial resolution allow one to connect to galaxy scales. We can now look at some characteristics of the simulated galaxies and at their formation processes.

### 3. Morphology of Simulated Galaxies

Paper I describes the straightforward method of identifying simulated galaxies as high density baryonic objects using a friends-of-friends grouping algorithm. We also noted the formation of a substantial population of disk structures. In this section, we would like to examine further the morphological characteristics of the galaxy population. Shapes can be classified for the larger objects and compared to the observed type of elliptical, spiral, and irregular. With a resolution of order 10 kpc, only the large scale galaxy structures can be seen and little information will be provided on internal structure. Additionally, the SPH method imposes some strict limitations.

The most limiting aspect is that the baryons in the simulation are always treated as gaseous. A main effect of thermal and artificial pressure is to prevent interpenetration of gas clouds by shocking. In regions of high density and high pressure, not only strongly convergent flows, but also random motions, will be damped out. Gas dynamics strives for smooth flow fields with little dispersion. The two solutions are simply translation and rotation. One should expect the galaxy objects to have a bulk velocity and/or a rotational velocity with small internal dispersions.

This expectation has several consequences for morphological studies. Elliptical galaxies, whose shapes derive from the velocity dispersions of stars, will not be seen. Such objects in this simulation would have their internal motions damped and collapse into

high density lumps at the resolution scale. The rotational motions of spirals, however, can be simulated. Angular momentum in collapsing gas clouds will be preserved and disk structures can form. These objects, too, will have their dispersions reduced and will be smaller. Any halo component in the spirals will collapse to the unresolved scales. Irregular galaxies will follow the same pattern: random motions will damp to the resolution scale and aligned motions, such as rotation or tidal tails, will remain. Mergers and interactions between galaxies should strip mass either by ejection during encounter or via linear tidal features. A gaseous galaxy cannot be dispersed by pumping energy into internal motions. These limitations are inherent in the computational method. The inclusion of star formation will ameliorate many of these considerations and exacerbate others.

The formation of galaxies with disk structures was reported previously. An example of a disk galaxy with an infalling satellite is presented in Figure 3. The large object has a baryonic mass of  $1.5 \times 10^{11} M_{\odot}$  with a disk diameter of 18 kpc and the satellite contains  $1.2 \times 10^{10} M_{\odot}$  and is at about 40 kpc away. The dense central cores are partly numerical artifacts because the gas particles with random motions (i.e., the ones that might form a stellar bulge) have their orbits damped to this scale. Also note that the angular momentum and hydrodynamics have produced disks thinner than the softening length; a feature which aids recognition, but does not represent the true resolution scale of the disk.

An example of a tidal encounter is shown in Figure 4. The projection is face-on to the disk and the satellite's orbit is inclined about 30 degrees to this plane. As the satellite begins its orbit, leading and trailing tidal tails develop. The leading tail appears to accrete both onto the disk and into a small lump during a close pass. A long trailing structure is evident, its striking thinness is a numerical effect due to the lack of velocity dispersion in the satellite. Some comparison can be drawn to the Magellanic clouds where the Magellanic stream has been suggested to have been tidally stripped (Lin & Lynden-Bell 1982; Moore & Davis 1994). However, at large radii the simulated satellite has two tails while no leading tail for the Magellanic clouds is apparent. Within the disk galaxy, a ring structure appears to form in response to the satellite's orbit, but our resolution of such structure is marginal. The simulation has resolved not only galaxies, but also the interactions between galaxies and satellites. For those accustomed to cosmological simulations only producing large scale plots like Figure 1, the detail in this figure is remarkable.

There are other details in the simulation that should be noted not for their scientific merit, but for their complete lack of merit. The left panel of Figure 5 shows an extreme close-up of the second largest object. Note the fine structure resembling spiral arms. Such structure is completely unresolved and totally bogus. The scale of the core region in this figure is about 3 kpc, well below the resolution limit. On these scales, the gravitational force becomes constant and the pressure force drops to zero. The particles may appear to form structure, but it is in no way physical. The right hand panel of Figure 5 shows the same view on a scale four times larger.  $3.7 \times 10^{11} M_{\odot}$  of baryons have collapsed to an amorphous lump about 20 kpc by 10 kpc by 15 kpc. About 75% of this mass is concentrated within 2 kpc of the center. This is an example of an unresolved object. If star formation

were included, one might expect these galaxies to be supported by internal motions and resemble elliptical or lenticular galaxies.

All of the expected morphological types are present. Using a three dimensional visualization program, shapes have been examined for the 35 simulated galaxies with more than 300 particles. Each is classified as a disk, an unresolved lump, or a merger, and the local environment, cluster or field, is noted. The results are given in Table 1. The distribution changes considerably between field and cluster environments. The fraction of disks decreases from 86% in the field to 54% in cluster environments. These fractions compare to the observed morphology-density relationship which finds a spiral fraction up to 90% in the field and as low as 10% in the richest clusters (Dressler 1980; Postman & Geller 1984). Our poor cluster has perhaps a slightly enhanced spiral fraction relative to observations. Although the two mergers occurring at this output are found in the field, the disk abundances argue for more merging in cluster environments. One of the mergers clearly shows a satellite impacting a disk face-on and creating large waves throughout the structure. Many of the other disks have smaller amplitude warps. These occurrences mesh well with theoretical predictions that mergers will disrupt disks and imply more merging occurs where the disk fraction is low. One object in the central cluster shows a strong tidal elongation, having just recently passed by the most massive galaxy. Tidal features are more prevalent on the smaller mass objects in the simulation and not on these large ones. A diversity of structure is in evidence, only some of which has there been space to describe in this section.

#### 4. Galaxy Formation History

Having many outputs from the simulation, it is possible to trace the simulated galaxies throughout their evolution. To do this, we have examined the particles in each object found by the grouping algorithm over 21 outputs. The particles are tracked to find out which objects, if any, they reside in at the previous and next outputs. If a significant percentage of particles, taken here as 30%, are found in a previous or next object, then the two objects are linked together. In this manner one builds up a network spanning the outputs and can follow the growth of an object and the merging of objects by tracing the links. We also tracked the infrequent instances when an object split into two pieces or disappeared from the object list. The split objects were actually two objects that made a close pass and were linked together by the grouping algorithm during the pass. Most often, they merged soon thereafter. Objects that disappeared from the list were small mass ones that temporarily fell below the minimum particle cutoff.

When an object appears on the list for the first time, it is considered to be newly formed. The top panel of Figure 6 shows a histogram of the formation of galaxy-like objects with baryonic masses  $M_B > 3.2 \times 10^9 M_\odot$ . The peak of formation at this mass scale occurs very early, only about  $10^9$  years after the Big Bang, with a roughly exponential decline in formation rate thereafter. Translated to redshifts, these small objects reach their

peak formation rate at redshift  $z = 4$ . Gaussian statistics predicts a tail of the collapse of very small overdensity perturbations continuing to  $z = 0$ , and such a tail is consistent with our data. The objects plotted in the histogram are the smallest resolvable objects in our simulation. Larger mass scales collapse later, as the hierarchy builds. Objects with  $M_B > 1.1 \times 10^{11} M_\odot$ , approximately the baryonic mass of an  $L_*$  galaxy for the assumed baryon fraction, have a later peak formation redshift of  $z = 2.5$ . This epoch is still only  $2 \times 10^9$  years after the Big Bang and over  $10^{10}$  years before the present day in this cosmology. Galactic structures can form in a relatively short time compared to their ages.

The bottom panel of Figure 6 shows the merging histogram for these objects. A merger is counted when two objects trace to the same object at the next output. If more than two objects merge into one object, extra events are counted. As expected for hierarchical clustering, the peak of merging is delayed with respect to the peak of formation. Notice that the merging peak occurs at about the same time as the formation peak of objects 30 times more massive. If merging were the dominant process for increasing mass, one would expect the merging peak to coincide with the formation peak of objects only a few times more massive. Clearly, accretion of mass which is not in collapsed objects is more important for building these objects than merging. Merging also occurs more stochastically than formation with more variance in the histogram. The peak in the merger rate at  $z = 2.2$  can be identified with the collapse of filaments around the central cluster and the formation of the central object of the smaller group (see Figure 1). The later merging peaks at  $z = 1.5$  and  $z = 1.1$  are correlated with the periods of heaviest infall through the center of the central cluster. These observations suggest that merging is heavily linked to group and cluster formation, while accretion is the dominant process for adding mass to galaxies.

The above discussion concerns the initial formation of objects at one mass scale and does not relate the objects to their final states. Certainly, one does not expect a  $10^{10} M_\odot$  object at  $z = 5$  to have no mass accretion and retain that same mass today. All of the simulated galaxies at the final output are traced back to their earliest forming resolved progenitor. Figure 7 shows the resulting correlation between redshift of formation (or first appearance),  $z_f$ , and the final mass. Such a trend would follow from a simple accretion argument: objects which form earlier have a longer time to accrete and end up with larger masses. However, the mass accretion rates for these objects are not constant over time (Paper I, Fig. 13) and such reasoning is oversimplified. The correlation also reflects the tendency for early forming objects to be in regions of higher density on larger scales. Thus, high redshift objects have both more time and more mass with which to build to larger mass scales.

This relationship between earlier formation and higher mass provides consistency amongst other results. Cen & Ostriker (1993), using a lower resolution simulation with heuristic galaxy formation, also reported a trend that the earliest forming objects ended up in the densest regions. Previously, we reported that the more massive objects are likely to be found in the denser environments of the simulation (Paper I, Fig. 10). Combining



these results and the one above, we see that our high resolution run confirms the Cen & Ostriker result and goes further to show a correlation of both mass and formation redshift with local galaxy density. Extending these ideas, one notes that larger mass and older age (higher  $z_f$ ) correlate to earlier Hubble type. The formation of early type galaxies predominantly in higher density environments was confirmed by the morphological studies in §3. Thus, hierarchical structure formation naturally agrees with the trends in mass, age, and morphological type in the observed morphology-density relation.

## 5. Disk Formation and Hierarchical Collapse

Galaxy formation is inherently a complex, dynamical, three dimensional process. Much of the intuition for the process is gleaned by examining visualizations of the simulation on a computer screen. A characteristic pattern of disk formation emerges from studying the process for the well resolved objects. Disk formation will be presented by studying one example in detail. This example is typical in that it highlights the important points in a relatively straightforward way. Much more information is contained in the three dimensional and kinetic aspects, but these figures provide the essential flavor of the disk formation process. Other objects show variations on this theme.

### 5.1. *The Formation Process*

Figure 8(a,b) provides a time sequence of the collapse of the sixth most massive galaxy. Within a radius of 50 kpc, the total mass is  $1.2 \times 10^{12} M_\odot$  and the baryonic mass is  $2.0 \times 10^{11} M_\odot$ . Note that the virial radius is much larger at 171 kpc, and contains total mass  $2.4 \times 10^{12} M_\odot$  and baryonic mass  $2.7 \times 10^{11} M_\odot$ . The panels show only the baryonic particles in 200 kpc cubic regions at approximately 215 Myr intervals. Velocity vectors are plotted as tails. The late evolution of this object has been presented in the tidal encounter of Figure 4.

Being a large object, a perturbation is apparent at high redshift. By  $z = 6.62$  a strong filament has formed with an underdensity to the left in this projection (XZ). This collapse region is the middle section of the long filament in the lower right of the first panel of Figure 1 (a YZ projection). Following the evolution in Figure 1, one can see that the section of filament below this region forms another galaxy and the section above it flows into the central cluster. The bifurcations of the velocity field are apparent in the  $z = 9.0$  panel, but quickly expand beyond the box size.

Skipping for a moment to Figure 9, we show two projections of a 400 kpc box about the object at  $z = 6.62$  with circles around the particles that end up in the densest region at the final output. The filament segment is clearly marked in the XZ projection (left panel) and seen end-on in the XY projection (right panel). Note also that the distribution is simply connected, but highly asymmetrical, indicating that spherical clouds are a poor approximation in hierarchical formation. Indeed, the XY projection indicates a grid of smaller filamentary structures that will collapse first and then combine with the main perturbation.

Continuing with Figure 8, the  $z = 5.28$  and  $z = 4.41$  panels show the collapse of the filament segment along its axis. Such a collapse is mostly one dimensional and contains little angular momentum. This sequence of filament formation, segmentation of the filament, and collapse of the individual segments is apparent not only on galaxy scales, but also on much more massive scales in larger volume cosmological simulations. Hierarchical collapse may be loosely characterized as a fractal collapse of filaments progressing from small scales to large.

On the heels of collapse along the filament axis comes the infall of the smaller nearby structure from the right in the  $z = 4.41$  through  $z = 3.32$  panels. This material is from the smaller filaments apparent in Figure 9. Much of the structure has collapsed into several small clumps, of which the two largest appear at the bottom of the plots. The smaller clump enters the region from the back right corner while the larger's orbit is roughly in the plane of the projection. The central object has little vorticity until these gas clouds fall into orbit, dissipate inward, and dominate the flow field. By the time the smaller one has accreted,  $z = 2.20$ , a clear disk with a smooth flow field has been established. While the large cloud does not impact the inner regions, its gravitational presence does aid disk formation and the plane of the disk is at an angle intermediate to the orbital planes of the small and large clumps. Though not clearly seen in this projection, continuous infall comes from many different directions, is slowed by shock heating, and softly accretes onto the disk.

The process shown in this example is common to disk formation in the simulation. The robust elements are the formation of a filament, the collapse of the filament, infall of a few dense clouds to build a basic disk structure, and slow accretion of low density material to strengthen the disk. The angular momentum arises naturally during the collapse from the tidal fields of neighboring perturbations. Bifurcations in the gravity field leave irregularly shaped regions that collapse with significant angular momentum. Galaxies that do not form disks deviate from this process. Some form near the vertex of several small filaments and have mostly radial (small impact parameter) cloud accretion. Others encounter the hot gas in group or cluster environments and have their surrounding gas heated to the inefficient cooling regime and/or stripped.

## 5.2. *The Resulting Structure*

To illustrate the structure of the resulting disk galaxy, Figure 10 shows averaged radial profiles of several quantities out to 100 kpc. The gas density falls as a power law with  $\rho_{\text{gas}} \propto r^{-2.8}$  while the total density (not shown) follows  $\rho_{\text{tot}} \propto r^{-2.4}$ . The density spike at 60 kpc indicates the satellite galaxy and is very prominent because the points are mass weighted averages. The temperature is near the minimum cutoff value in the dense inner regions and quickly rises to the virial temperature. The mass profiles show that the baryons dominate the mass on scales close to the resolution limits and only reach the cosmic proportion at about 100 kpc. Last, the radial dependence of the smoothing length is provided to remind the reader of the variable resolution of the hydrodynamics.

Resolution is proportional to  $\rho^{-\frac{1}{3}}$ , making the effective radii of particles larger in the low density regions. These profiles are very similar in all the well resolved disk objects and agree with those of Navarro & White (1994).

The components of this simulated galaxy form a neat and stable picture. At the interior is a rotationally supported disk with baryons dominating the central mass and falling off more sharply than the total mass. Enveloping this is a  $10^6$  K isothermal gas halo which extends ten times larger than the cooled region and contains about half of the baryonic mass within the virial radius. Finally, there is a dark matter halo providing the dominant mass and which is in cosmic proportion with the baryons at large radii of the system. The structure of this object is basically unchanged for another 1800 Myr through the end of the simulation and presumably would remain so until a merger with a galaxy of comparable mass or interaction with an intracluster medium could perturb it.

Such structure is oversimplified by the numerical model. The stellar bulge is missing for reasons described above and other physics of galaxies is either smoothed or not included. The size of the disk is likely decreased from its natural size because of numerical effects, however, the factor of ten scale difference between the disk and halo fits theoretical expectations. And the implication that a significant amount of baryonic mass resides in a gaseous halo is certainly intriguing. Overall, the correspondence to the analytic picture of a dark matter dominated galaxy is relatively strong.

### 5.3. Analysis of the Process

The above picture of disk formation is quite different from the simple spherical collapse model. The distribution of matter is decidedly not spherical nor uniform. The collapse is also not coherent nor synchronized, but occurs in many places with simultaneous formation on several scales. In addition, only a small homomorphic collapse of the disk is required for it to be rotationally supported, not the large factor envisioned by the simple model. Finally, the angular momentum is not smoothly distributed throughout the collapsing protogalaxy, but, as shown below, becomes dominated by the motions of a few objects. The spherical collapse model greatly oversimplifies the rich complexity of the collapse process.

The development of the angular momentum in the system is interesting. The origin of angular momentum in galaxies is usually attributed to tidal torques in the surrounding gravitational potential. One can see the process occurring early on in the figures. The fracturing of the gravity field leaves an irregularly shaped and unevenly structured collapse region that will naturally develop angular momentum when collapsing in a tidal field. In Figure 11, we show the development of the spin parameter in the system, defined as  $J|E|^{1/2}G^{-1}M^{-5/2}$  where  $J$  is the angular momentum,  $E$  is the total energy,  $M$  is the mass. Most of the angular momentum in the baryons (top panel) is concentrated in the two clouds, which show as distinct peaks of the curves. When they accrete, their rotation is deposited over the inner regions. The dark matter spin parameter (bottom panel) remains near the same magnitude throughout. A small effect from the clouds is apparent, but it washes away and the entire dark matter curve at  $z = 1$  is  $\lesssim 0.1$ . Figure 11 affirms the

visual intuition one gets for the development of the angular momentum of the system from Figure 8.

The emergent picture of disk formation is one dominated by discrete accretion of gas clouds. Disks arise from infall of individual dense gas clouds that carry most of the angular momentum of the system. These clouds can dominate the flow because they have formed at large radii and infall with large impact parameters; thereby combining significant mass, linear momentum, and angular momentum. Additionally, the matter in the small filamentary structures begins to collapse together while infalling. Hence, infall directions, and thus, angular momentum vectors, are somewhat correlated. Though more mass is accreted in low density material, this material does not have large, compact momentum and is slowed before it can directly impact the inner regions. This soft accretion adds to the mass of the disk, but does not establish a flow pattern. Galaxy formation in hierarchical models invokes the idea of disk formation by discrete accretion.

The emphasis on merging for building a galaxy in hierarchical structure formation has called into question the ability to form disk structures and their stability after formation. If the merger events were numerous, the chance for correlated angular momentum would be low and late mergers would heat and destroy a disk. However, hierarchical structure formation requires only a few significant events to build the galaxy. The next level would be a merger with an object of similar size, not a continuing rain of smaller objects. For those objects in the simulation which do experience many mergers, resolved disks do not form. We also see encounters where satellite galaxies impact on already formed disks and strongly disrupt them. The high fraction of disk morphologies indicates that these are the exceptions, not the rule. This simulation demonstrates that galactic disks not only form in abundance within hierarchical models, but also can survive for several times  $10^9$  years.

To engage in a bit of speculation, one may directly identify stages of the collapse process with the structure in spiral galaxies. The collapse along the filament axis produces little angular momentum and would characteristically form a halo component. Subsequent stellar accretion, which cannot be differentiated in this simulation, would build a halo in the pattern of that described by Searle and Zinn (1978). The cloud infall to establish a disk would have significant dispersion, some internal to the clouds and some created in the process of defining a rotation plane, that might lead naturally to a thick disk. Later gas accretion and settling would be softer and more coherent: producing a thin disk component. Although we have neither the physics to simulate a halo nor the resolution to differentiate disk components, the picture fits with observed galactic structure and flows naturally from the dynamical processes.

A healthy skepticism will naturally ask how this formation process is affected by the simulation limitations. The main point on this matter is that as long as the baryons remain gaseous, the simulation is correct. The infalling gas clouds have enough linear and angular momentum that their ram pressure on the gas in the inner regions produces the vorticity seen. Artificial pressure effects will, if anything, understate the ram pressure

since the clouds will be slowed in advance of shocks by the finite resolution of the code. For the example above, the densest baryons will likely have formed stars and thus become collisionless, but this will only occur in the inner 10 kpc of the forming galaxy and the central regions of the large cloud. Densities in these regions exceed  $1 \text{ cm}^{-3}$  while the small cloud is of order  $10^{-2} \text{ cm}^{-3}$ . Star formation might allow the large cloud to orbit with less drag, but should not change the path and angular momentum transfer of the small cloud.

If star formation proceeds efficiently in the infalling clouds, it is difficult to envision how hierarchical structure formation will produce an abundant population of disks. The linear collapse of filaments does not produce much angular momentum. The gravitational influence of satellite orbits would be inefficient at transferring angular momentum, especially to the inner regions. Angular momentum would arise mostly from the slow accretion of low density gas. However, because the angular momentum of this gas is not well correlated, it may be unable to dominate the dynamics. It seems imperative that infalling clouds be gaseous for hierarchical collapse to produce disks.

## 6. Discussion

This paper has presented a coherent picture of galaxy formation within hierarchical structure formation models. An early formation epoch is observed, with the peak formation rate on the  $10^{12} M_{\odot}$  scale occurring at  $z \approx 2.5$ . Formation rate after peak drops with an exponential tail while merger rates increase, though mergers tend to be dominated by cluster interactions. The range of morphologies observable in the simulation are a good match to observed types and include rotationally supported disks and extended tidal tails. The structure of the disk galaxies consists of a gas disk extending tens of kpc surrounded by both hot gas and dark matter halos out to ten times larger. Hierarchical structure formation is quite successful at forming reasonable galaxies.

The observed morphology-density relationship appears as a natural result of hierarchical formation. In Paper I, we noted that massive galaxies resided in the denser environments of the simulation. We show here a strong correlation between mass and early collapse, indicating that massive objects are older. Finally, direct examination of morphologies shows that disk galaxies are more prevalent in the field. Equating disks to spirals and higher mass and older age to ellipticals, the trends in mass, age, and morphology agree with the observed morphology-density relationship.

A new method for making spiral galaxies arises in hierarchical structure formation. The importance of merging was noted by Navarro & White (1994) and here we hone the details of the process. The early stages are characterized by large and small filamentary structures which collapse separately. The angular momentum transport is dominated by a few gas clouds which can punch through a gas halo, directly impact the inner regions, and establish a flow pattern. Disruption of the disk from too many mergers is avoided because only a couple significant accretion events are required to build a level of the hierarchy. Because ram pressure is important for transferring angular momentum, the timing of star

formation during this process will be a key ingredient. Further studies will be needed to probe deeper into this process of disk formation by discrete accretion.

One strong conclusion is that, in hierarchical structure formation, there is no such thing as a simple spherical collapse. The collapse of a galaxy sized mass is more chaotic than uniform, with separate pieces undergoing local collapse simultaneously within the global picture. Ideas of sphericity and uniform distribution of angular momentum are inconsistent with the findings. While the simple model is no doubt analytically useful, its practical utility when applied to hierarchical structure formation should be evaluated.

If we indeed live in a hierarchical universe, the above results have several implications for galaxies. The halos extend approximately 10 times larger than the luminous parts of the disks. Rotation curves should be flat or only mildly falling, and certainly not Keplerian, within radii of about 150 kpc. Such a halo size estimate fits well with that predicted from observed mass to light ratios (Bahcall, Lubin, & Dorman 1995), although the conclusions of those authors suggest a low density universe and our simulation assumes a flat universe. On the lower bound, HI observations indicate a cool gas extent several times the optical disk (e.g., Cayatte et al. 1994) and the need for a dark matter halo already several times more massive than the maximal disk at radii around 30 kpc (e.g., Begeman 1989). The gas in these large halos is roughly isothermal at a temperature of a few times  $10^6$  K and contains one third to one half of the baryonic mass within the virial radius. At densities near  $10^{-3} \text{ cm}^{-3}$  the total free-free emission is about  $5 \times 10^{41} \text{ erg s}^{-1}$  peaked at a couple hundred eV. Such emission is not strong enough to be seen in the bandpasses of current X-ray satellites (see also Navarro & White 1994). In the simulated galaxies, the halo gas cools in the inner regions and provides a continual source of mass accretion onto the disk. However, as the simulations do not include interactions between the disk and halo (galactic fountains, ionizing radiation), such accretion is not a firm prediction.

The correlation between an object's merging history and its final morphology is not completely straightforward. Objects with lots of merging and recent merging do not form disks. A quiescent merger history for a field object is a good indicator of disk formation. However, in the cluster, a quiet history does not always lead to a disk. Tidal perturbations can disrupt disks that have already formed, while heating and stripping of halo gas via interaction with the intra-cluster medium can interrupt accretion onto disks that are forming.

Probing the morphological information, one can explore the idea that ellipticals form from mergers of spirals. For the central galaxy of the cluster, which has the characteristics of a cD, formation is dominated by a series of merger events that occur early. The objects which merge do not have time to develop disks. A couple other objects that are candidates for ellipticals also form from several relatively quick mergers where disks do not form first. We also see a couple instances where formed disks are disrupted, though these may be fairly considered as interacting galaxies. Thus, the general trend is that our results do not support the idea that all galaxies form disks with ellipticals forming as mergers of disks.

Hierarchical collapse in dense regions progresses through the mass scales too quickly and with too much merging for disk formation. These conclusions are, however, drawn from only a handful of cases. Further, we have no handle on addressing dwarf ellipticals.

Having identified some characteristics of hierarchical formation, it is useful to consider whether such ideas could translate into observables. Figure 1 suggests that voids are more spatially stable than overdensities as features of the density field. The method for reconstructing the initial density field of Weinberg (1992) might provide additional insight if focused on the low density regions as well. Section 5 points out that filaments exist on all scales and that collapse progresses from small to large. One may find a useful measurement of the level of collapse in either the smallest filament which has yet to collapse or in the largest filament that has had time to form. Such a measure would be spatially variable and could provide an assessment of the local dynamical state in the mildly non-linear regime. The difficulty would be in extracting real space filaments from redshift space data.

This study of galaxy formation has provided numerous insights, but leaves many topics left to pursue. The presence of the cluster in the constrained initial conditions skews the formation process a bit. The average redshift of formation is assuredly higher in this overdense region. Perhaps the strong filaments which intersect at the cluster overemphasize the role of filaments in the galaxy formation process. Also, we can resolve formation for galaxies of mass scale  $10^{12} M_{\odot}$ , the process may differ for smaller masses. Both of these arguments are countered by noting that filaments are found on all resolvable scales and appear to be a ubiquitous part of the process. Resolution and unconstrained initial conditions will help settle these questions.

Another point is that the simulation finishes at redshift one. The early formation epoch for galaxies begs the question of what will happen at late times. Will the galactic disks remain stable for another  $8 \times 10^9$  yr? In the simulated region, most of the objects would end up in the cluster, where disk stability is questionable. For more general regions, the formation epoch would be later and the process may proceed slower, but disks would still need to be stable for a considerable fraction of the Hubble time. As seen in this simulation, the early fracturing of the gravitational field breaks the mass into distinct regions which collapse relatively quickly. Small objects near large galaxies become satellites as seen in the figures. There does not appear to be a large reservoir of disrupters available for late time infall. Small objects which do form later would be in other regions. These extrapolations of the current simulation favor disk stability with the acknowledged exception of galaxy-galaxy interactions. A random region can be evolved to the present day to check the arguments.

The effects of varying the cosmology should not be great. By focusing on small scales and not including the global aspects of the cosmological model, only hierarchical structure formation has been tested here. Changing the  $\sigma_8$  normalization will essentially just rescale the redshifts assigned to the simulation and perhaps speed up or slow down the processes. Using a low density universe may have the largest effect in that it forces structure formation

to occur early and then suppresses further growth. Such suppression may be required to maintain stable disks to the present day if the arguments of the preceding paragraph do not hold or if galaxy mergers are too frequent. Also, the reduced total mass and larger baryon fraction in low density and cosmological constant dominated universes will favor smaller galaxy halos and a quieter velocity field for the same luminosity. These changes may alter such aspects as the relative importance of interacting galaxies, but the basic hierarchical process should remain.

The ability to address simulations of galaxy formation within a cosmological context has been attained only recently. This study presents only a few of the qualitative and quantitative insights into the galaxy formation process that can be gained. The prospects for examining a wide range of characteristics of the galaxy population as it develops over a Hubble time are quite good.

The author wishes to thank Gus Evrard, Marc Davis, and David Spergel for helpful discussions. Support for this work was provided by NSF grant AST-8915633 and NASA grants NAGW-2448 and NAG5 2759. Computing resources provided by the San Diego Supercomputing Center and the Pittsburgh Supercomputing Center are gratefully acknowledged.



## References

- Bahcall, N. A., Lubin, L., & Dorman, V. 1995, ApJ 447, L81
- Barnes, J. E., & Hernquist, L. 1992, ARA&A 30, 705
- Begeman, K. 1989, A&A 223, 47
- Cayatte, V., Kotanyi, C., Balkowski, C., & van Gorkom, J. H. 1994, AJ 107, 1003
- Cen, R., & Ostriker, J. P. 1993, ApJ 417, 415
- Dressler, A. 1980, ApJ 236, 351
- Efstathiou, G., Bond, J. R., & White, S. D. M. 1992, MNRAS 258, 1p
- Efstathiou, G., & Silk, J. 1983, Fund. Cosmic Phys. 9, 1
- Eggen, O. J., Lynden-Bell, D., & Sandage, A. R. 1962, ApJ 136, 748
- Evrard, A. E. 1988, MNRAS 235, 911
- Evrard, A. E., Summers, F J, & Davis, M. 1994, ApJ 422, 11 (Paper I)
- Gott, J. R., & Thuan, T. X. 1976, ApJ 204, 649
- Katz, N., Hernquist, L., & Weinberg, D. H. 1992, ApJ 399, L109
- Katz, N., & Gunn, J. E. 1991, ApJ 377, 365
- Katz, N., Weinberg, D. H., & Hernquist, L. 1996, ApJS, submitted
- Kauffmann, G., White, S. D. M., & Guiderdoni, B. 1993, MNRAS 264, 201
- Lacey, C., & Cole, S. 1993, MNRAS 262, 627
- Lin, D. N. C., & Lynden-Bell, D. 1982, MNRAS 198, 707
- Moore, B., & Davis, M. 1994, MNRAS 270, 209
- Navarro, J. F., Frenk, C. S., & White, S. D. M. 1994, MNRAS 267, L1
- Navarro, J. F., & White, S. D. M. 1994, MNRAS 267, 401
- Postman, M., & Geller, M. J. 1984, ApJ 281, 95
- Rees, M. J., & Ostriker, J. P. 1977, ApJ 179, 541
- Searle, L., & Zinn, R. 1978, ApJ 225, 357
- Silk, J. I. 1977, ApJ 211, 638
- Steinmetz, M., & Mueller, E. 1994, A&A 281, L97
- Summers, F J 1993, Ph.D. Thesis, University of California at Berkeley.
- Toomre, A., & Toomre, J. ApJ, 1972 178, 623
- Tóth, G., & Ostriker, J. P. 1992, ApJ 389, 5
- Weinberg, D. H. 1992, MNRAS 254, 315
- White, S. D. M. & Frenk, C. S. 1991, ApJ 379, 52
- White, S. D. M. & Rees, M. 1978, MNRAS 183, 341

**Table 1**

Morphological Fractions by Environment

---

---

Morphology	Field		Group/Cluster	
	#	%	#	%
Disk	19	86	7	54
Unresolved	1	5	6	46
Merger	2	9	0	0

---

---

## Figure Captions

**Figure 1** – Time development of structure in the simulation. Positions of the dark matter particles within a slice of dimensions  $L \times L \times 0.2L$  are shown at six output times. The slice contains the principle collapse plane of the cluster that forms in the central region. For clarity, only one fourth of the particles are shown.

**Figure 2** – Dynamic range of the simulation. Plots of the dark matter (top row) and the baryons (bottom row) are shown in three successively enlarged regions at the end of the simulation. The left panel has dimensions  $0.4L \times 0.4L \times 0.1L$  and shows only one fourth of the particles. The center and right panels are cubical with side lengths of  $0.057L$ , and  $0.01L$ , show all particles, and are enlargements of the boxed area in the panel to their left. Physical dimensions of the region widths at  $z = 1$  are given on the plot. The left panel is a projection onto the YZ plane while the center and right panels are projections onto the XZ plane.

**Figure 3** – A disk galaxy with an infalling satellite in the simulation. All baryonic particles in the region are shown and perspective has been added by a visualization program. The disk is approximately 40 kpc across.

**Figure 4** – Tidal encounter sequence of satellite infall. The sequence begins in the upper left and proceeds left to right in each row. All baryonic particles in the region are plotted in a projection face-on to the disk. Panels are not equally spaced in time, but cover a total span of about 850 million years.

**Figure 5** – Unresolved hydrodynamic effects. The left hand panel shows the baryonic particles at the center of the second most massive galaxy in a cubical region 9 kpc on a side. The structure in this picture occurs below the resolution scale of the simulation and must be ignored. The right hand panel shows the same projection in a cubical region 40 kpc on a side.

**Figure 6** – Galaxy formation and merging histograms. The top panel shows the number of new galaxies found by the grouping algorithm at each output. The bottom panel charts the number of merger events (see text).

**Figure 7** – Correlation between formation redshift and mass. The redshift when a galaxy first appears in the simulation is plotted versus its final baryonic mass for the 215 galaxies found at the final output.

**Figure 8** – Time sequence of formation of the sixth most massive galaxy. Each panel shows the baryonic particles in a 200 kpc cubic region for the redshift indicated. The time interval between panels is about 215 Myr. Velocities are plotted as tails and are scaled such that 1000 km/s equals 0.15 of the box length or 30 kpc.

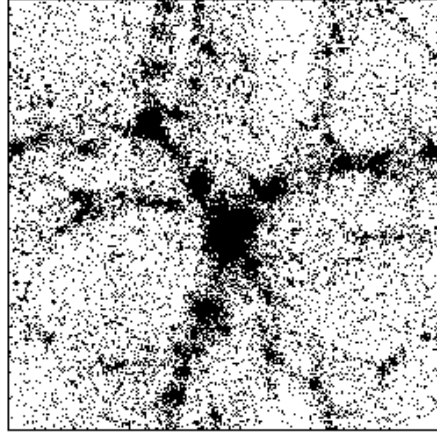
**Figure 9** – This figure shows a larger view of the  $z = 6.62$  panel of Figure 8(a). All baryonic particles within a 400 kpc cubic region are plotted and the particles which reside in the galaxy #6 at  $z = 1.01$  are marked by larger points. The left panel shows the same projection as Figure 8 (XZ) and the right panel shows a view approximately down the filament axis (XY).

**Figure 10** – Radial profiles of several quantities for galaxy #6 at  $z = 1.83$ . Values for density, temperature, and smoothing length are mass weighted average values in each bin. Mass profiles are mass interior to the bin and are marked by crosses for the baryons and circles for the dark matter.

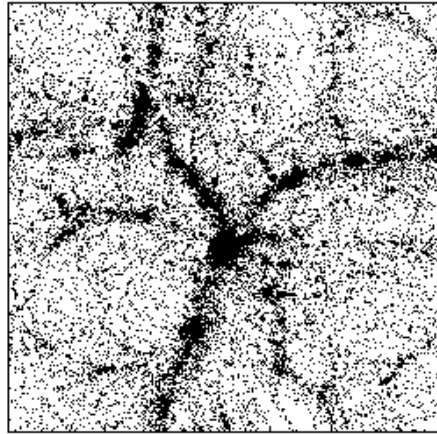
**Figure 11** – Spin parameter development. The dimensionless spin parameter (see text for definition) is plotted as a function of radius at several redshifts. The top panel is calculated from the baryons, while the bottom panel displays the curves for the dark matter.

## **Figures – Electronic Preprint Version**

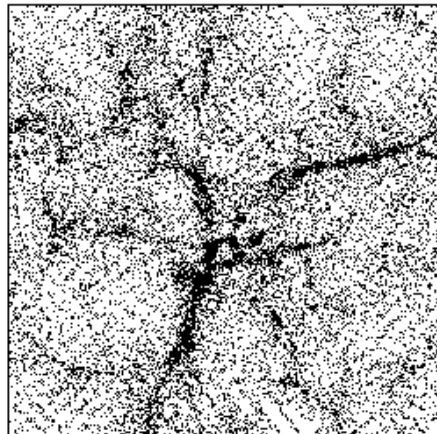
For the electronic preprint, the large figure files have been replaced with 100 dpi resolution scanned versions. Such processing reduces the file size and the printing time required while also increasing the compressibility of the files for electronic transfer. In this paper, the following figures have been replaced by scanned versions: 1, 2, 3, 4, 5, 8a, 8b, 9. Full resolution figures can be obtained from the author or from the WWW site: “<http://astro.princeton.edu/~summers>”.



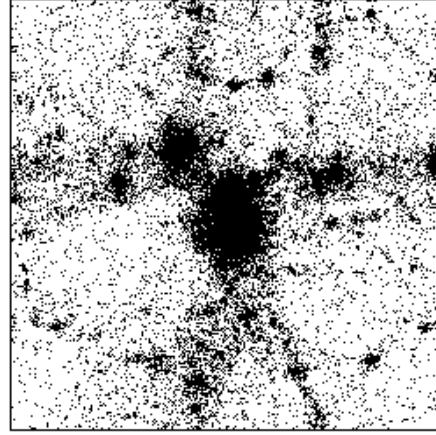
$z = 2.02$



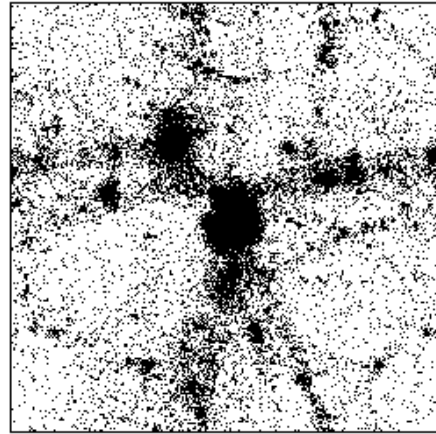
$z = 2.95$



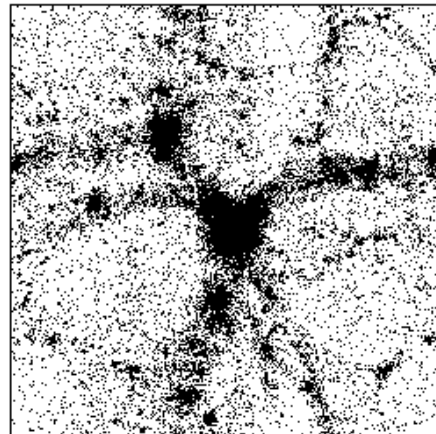
$z = 5.28$



$z = 1.01$



$z = 1.22$



$z = 1.58$

Figure 1

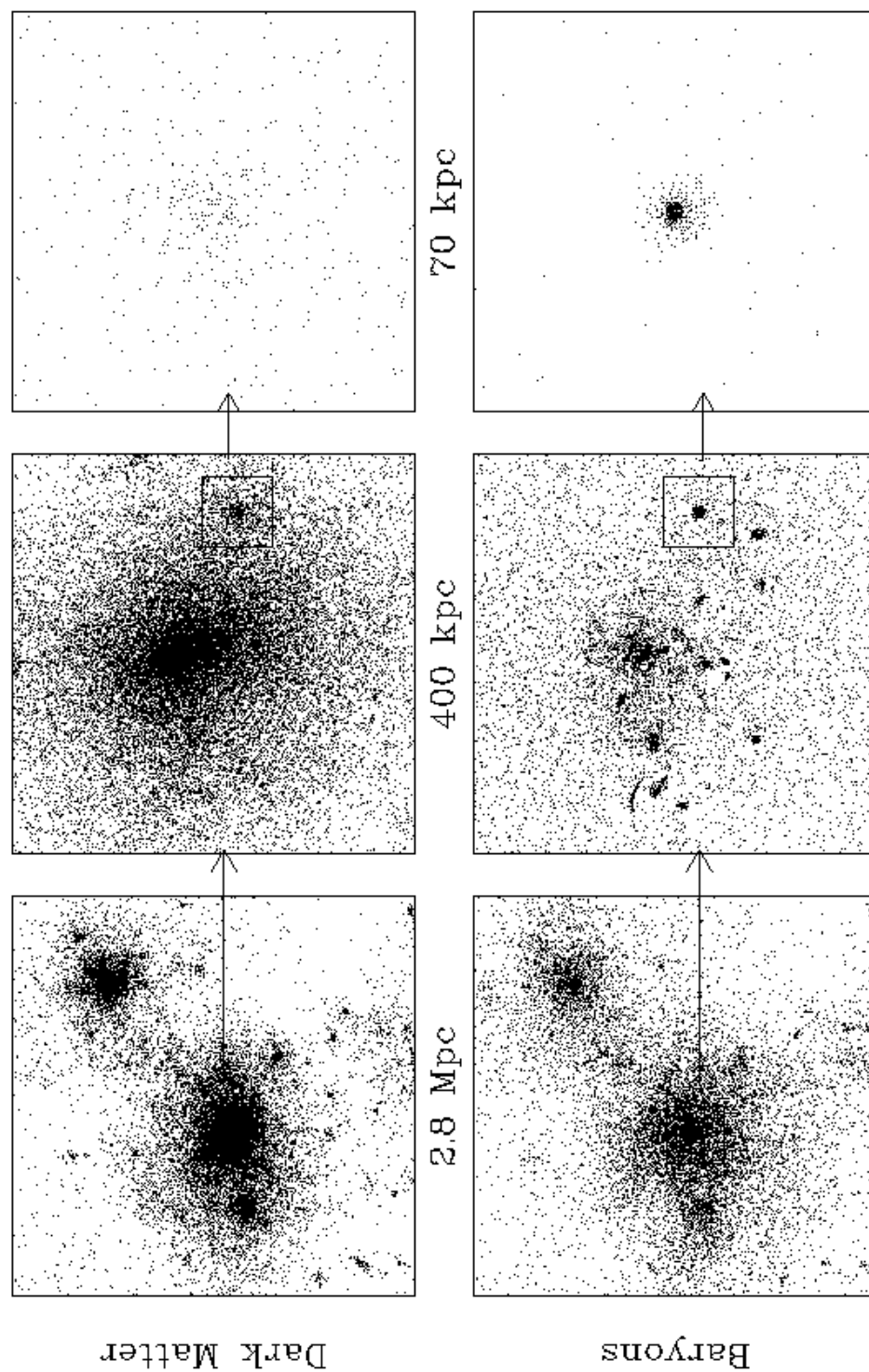


Figure 2

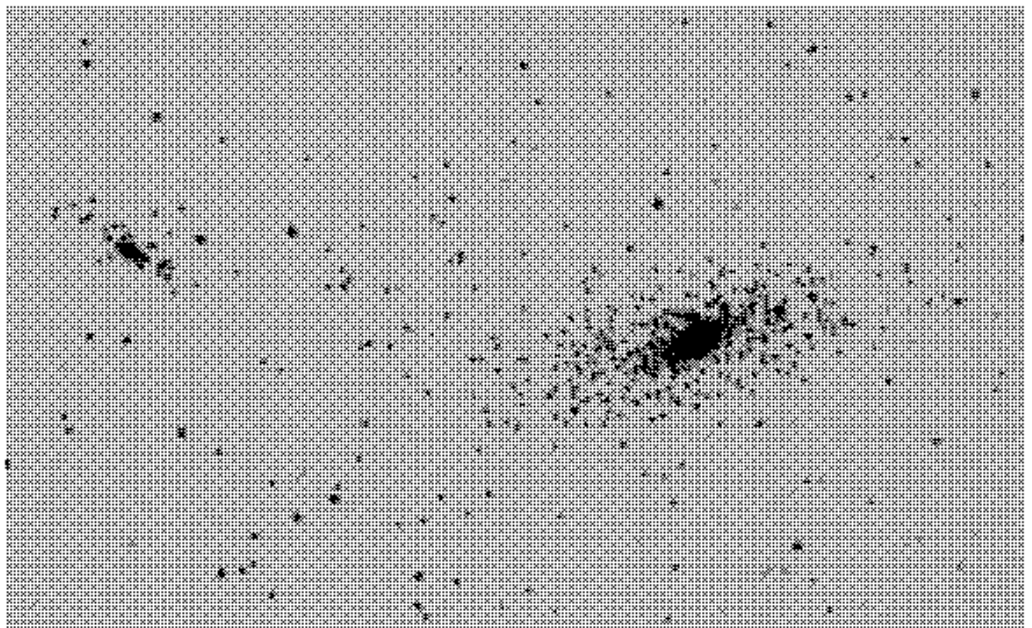


Figure 3



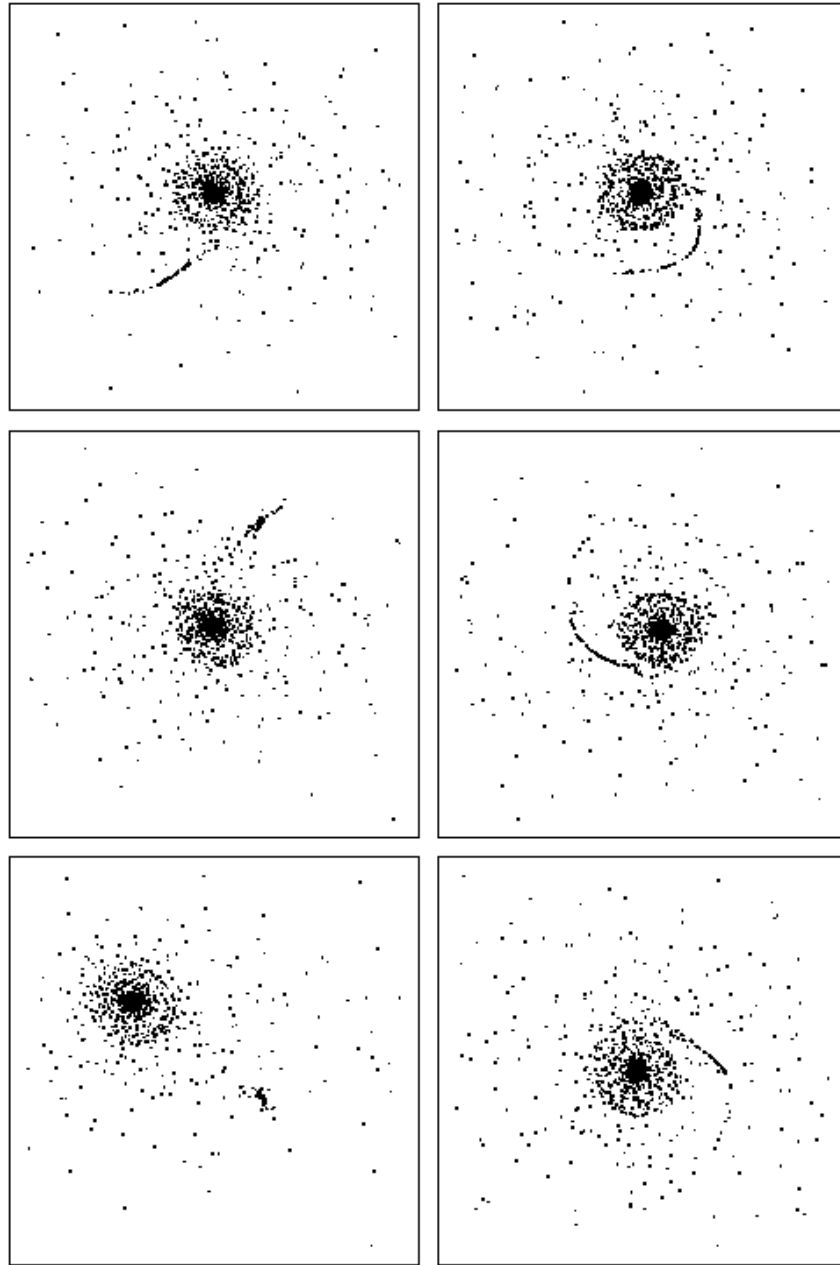


Figure 4

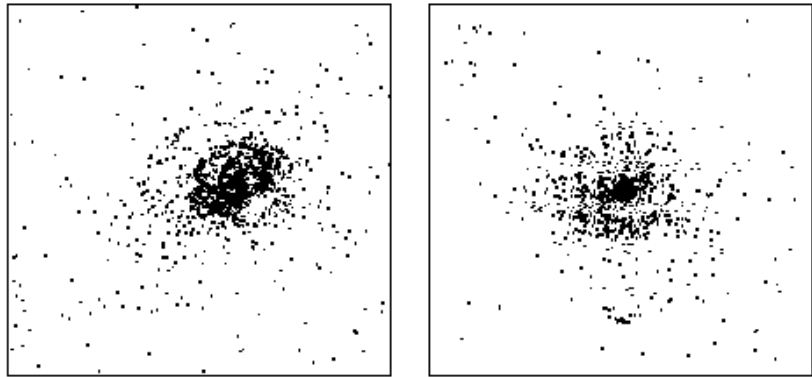


Figure 5

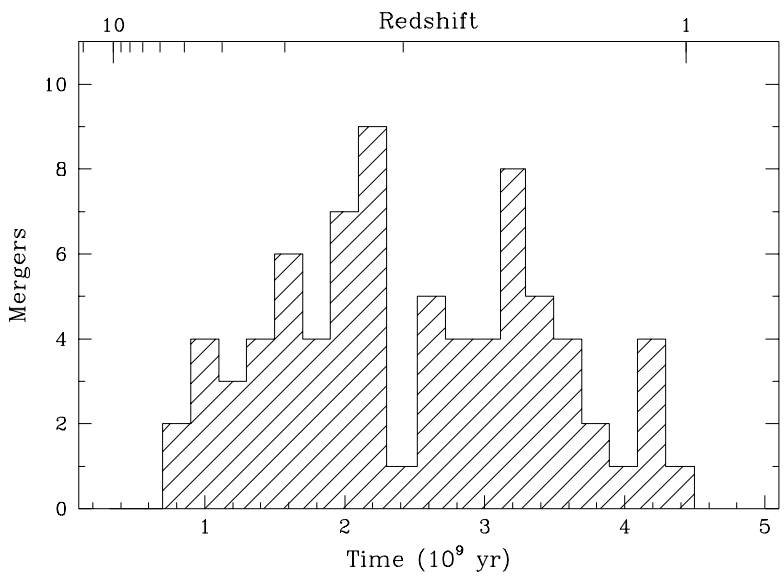
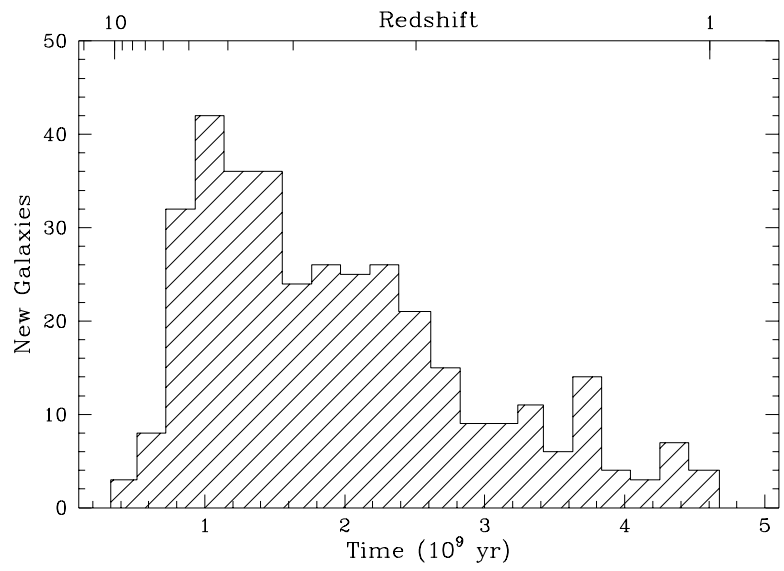


Figure 6

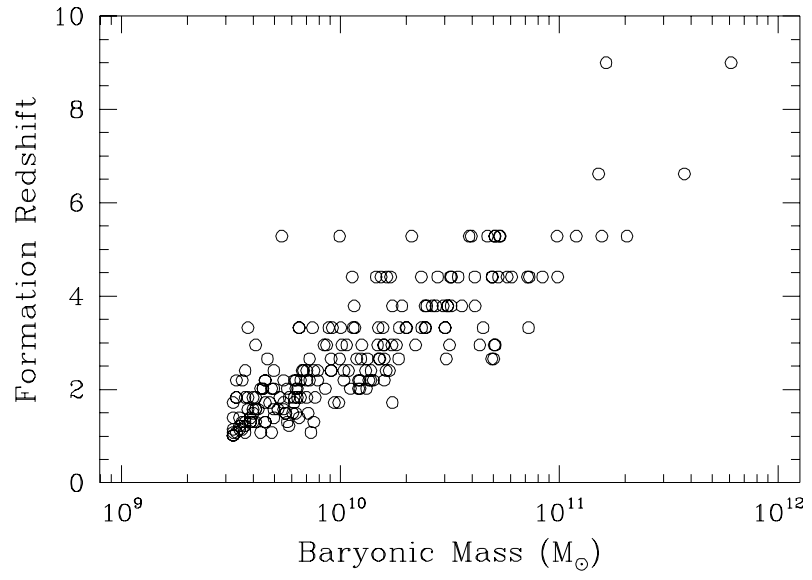


Figure 7

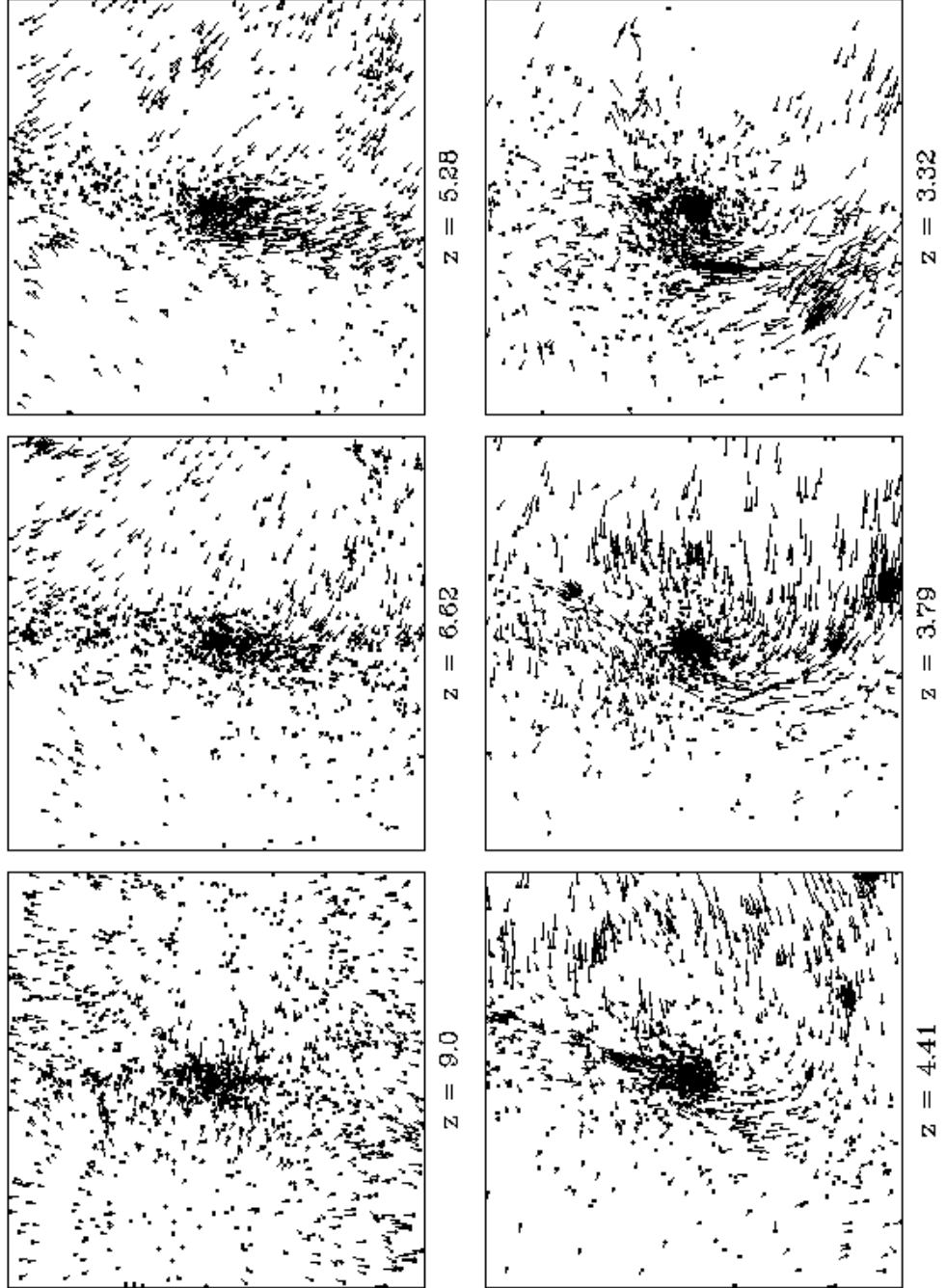
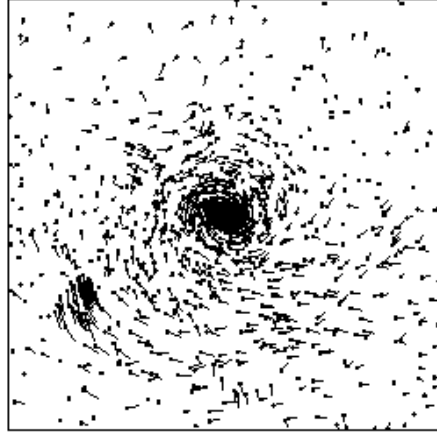
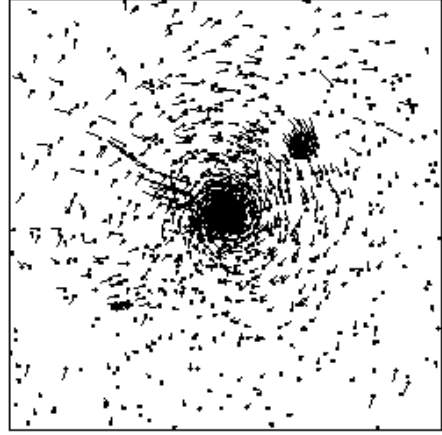


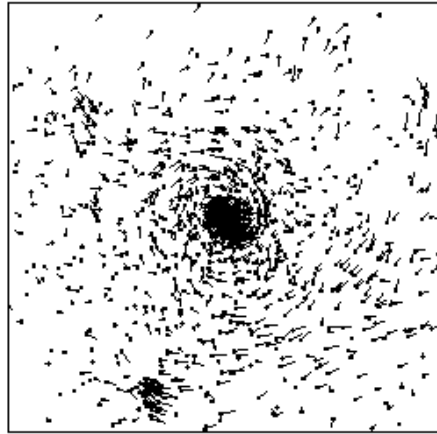
Figure 8(a)



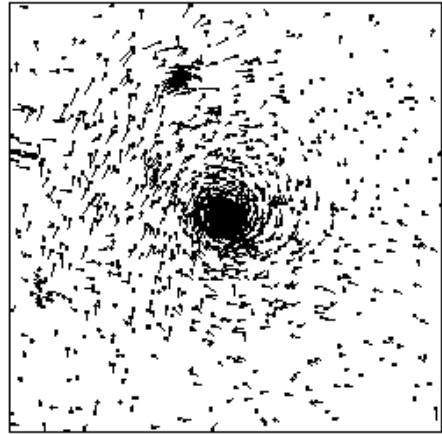
$z = 2.41$



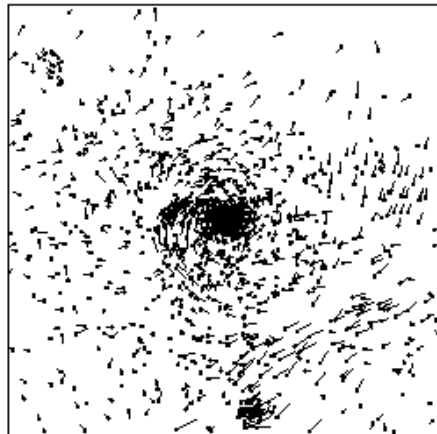
$z = 1.83$



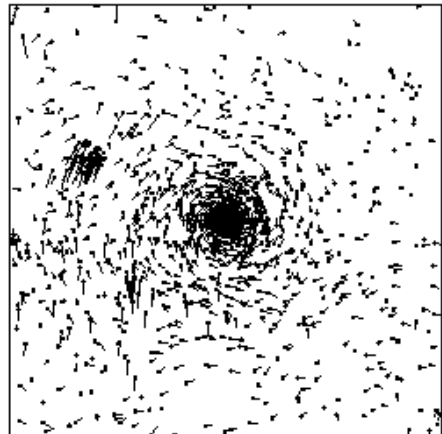
$z = 2.65$



$z = 2.02$

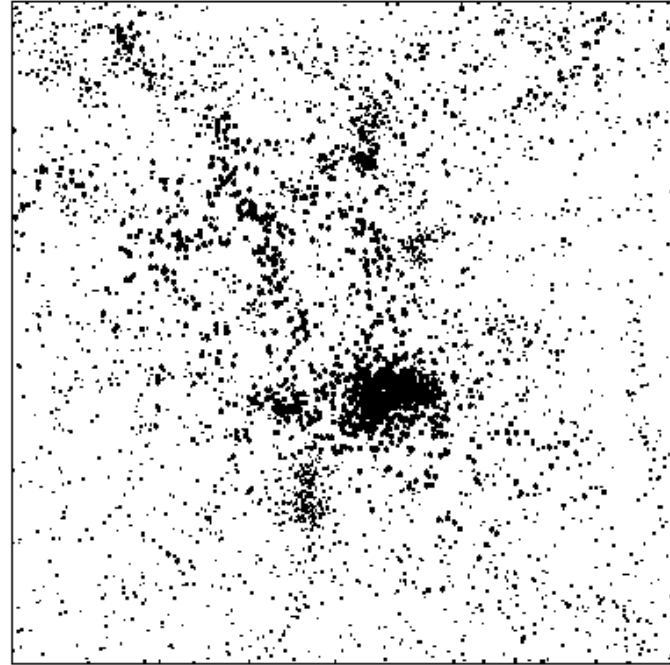


$z = 2.95$

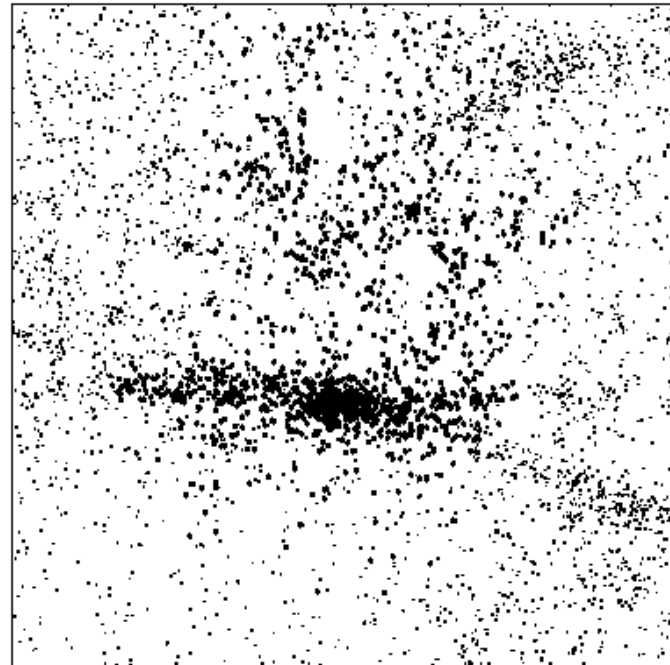


$z = 2.20$

Figure 8(b)



XY Projection



XZ Projection

Figure 9

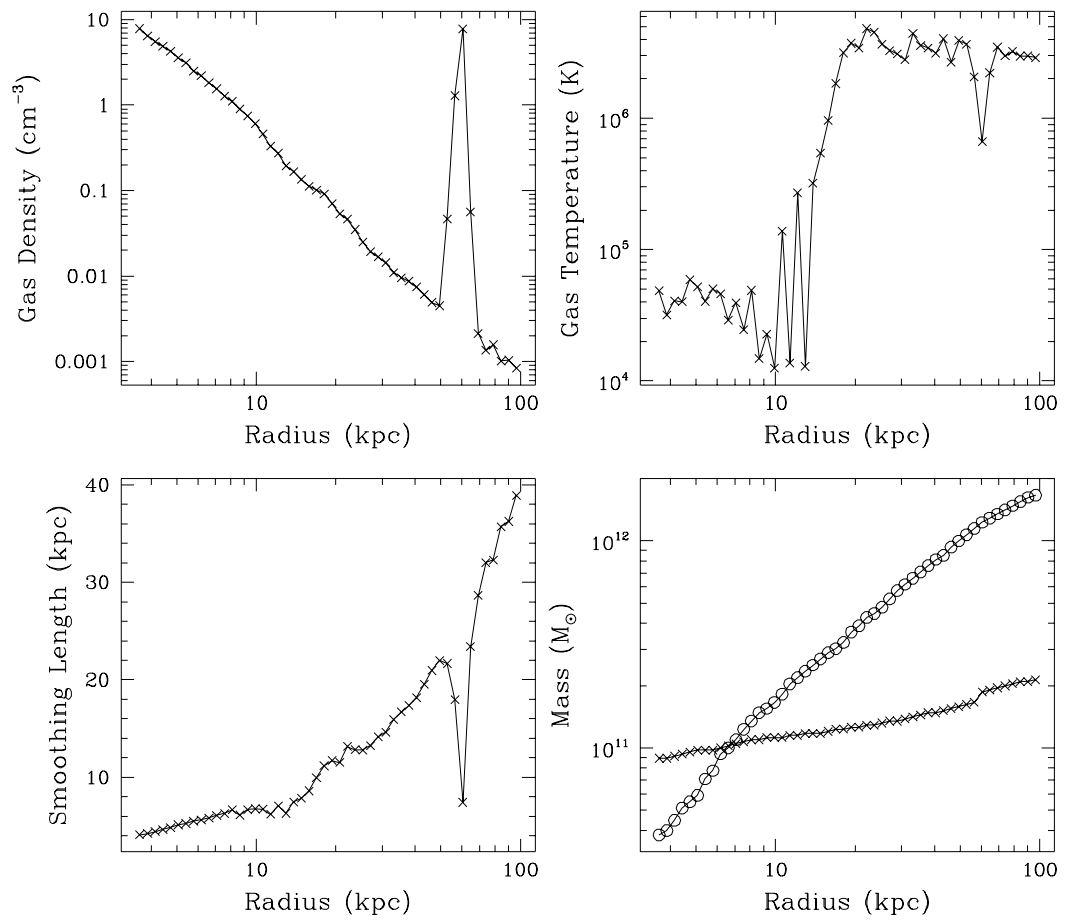


Figure 10



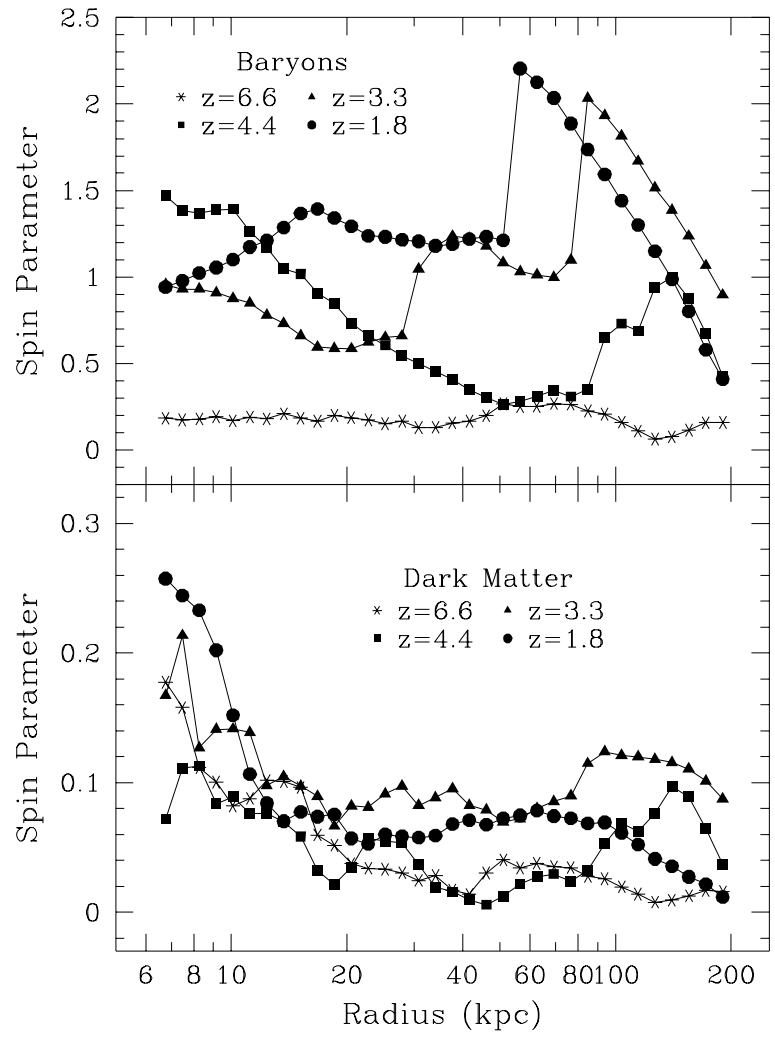


Figure 11